THE JOURNAL OF BIOLOGICAL CHEMISTRY VOL. 285, NO. 16, pp. 12101–12108, April 16, 2010
© 2010 by The American Society for Biochemistry and Molecular Biology, Inc. Printed in the U.S.A.

The Acyclic 2,4-Diaminopyrimidine Nucleoside Phosphonate Acts as a Purine Mimetic in HIV-1 Reverse Transcriptase DNA Polymerization*

Received for publication, December 18, 2009, and in revised form, February 11, 2010 Published, JBC Papers in Press, February 17, 2010, DOI 10.1074/jbc.M109.096529

Brian D. Herman[‡], **Ivan Votruba**[§], **Antonin Holý**[§], **Nicolas Sluis-Cremer**[‡], **and Jan Balzarini**[¶1]

From the [‡]*Department of Medicine, Division of Infectious Diseases, University of Pittsburgh, Pittsburgh, Pennsylvania 15261, the* [§]*Institute of Organic Chemistry and Biochemistry, Academy of Sciences of the Czech Republic, Prague CZ-16610, Czech Republic, and the* [¶]*Rega Institute for Medical Research, KU Leuven, Leuven B-3000, Belgium*

The acyclic pyrimidine nucleoside phosphonate (ANP) phosphonylmethoxyethoxydiaminopyrimidine (PMEO-DAPym) differs from other ANPs in that the aliphatic alkyloxy linker is bound to the C-6 of the 2,4-diaminopyrimidine base through an ether bond, instead of the traditional alkyl linkage to the N-1 or N-9 of the pyrimidine or purine base. In this study, we have analyzed the molecular interactions between PMEO-DAPym-diphosphate (PMEO-DAPym-pp) and the active sites of wild-type (WT) and drug-resistant HIV-1 reverse transcriptase (RT). Pre-steady-state kinetic analyses revealed that PMEO-DAPym-pp is a good substrate for WT HIV-1 RT: its catalytic efficiency of incorporation (k_{pol}/K_d) is only 2- to 3-fold less than that of the corresponding prototype purine nucleotide analogs PMEA-pp or (*R*)PMPA-pp. HIV-1 RT recognizes PMEO-DAPym-pp as a purine base instead of a pyrimidine base and incorporates it opposite to thymine (in DNA) or uracil (in RNA). Molecular modeling demonstrates that PMEO-DAPym-pp fits into the active site of HIV-1 RT without significant perturbation of key amino acid residues and mimics an open incomplete purine ring that allows the canonical Watson-Crick base pairing to be maintained. PMEO-DAPym-pp is incorporated more efficiently than (*R*)PMPA-pp by mutant K65R HIV-1 RT and is not as efficiently excised as (*R*)PMPA by HIV-1 RT containing thymidine analog mutations. Overall, the data revealed that PMEO-DAPym represents the prototype compound of a novel class of pyrimidine acyclic nucleoside phosphonates that are recognized as a purine nucleotide and should form the rational basis for the design and development of novel purine nucleo(s)(t)ide mimetics as potential antiviral or antimetabolic agents.

Acyclic nucleoside phosphonates (ANPs)[2] are nucleotide analogs that are characterized by the presence of a phosphonate group linked to a pyrimidine or purine base through an aliphatic linker (1). ANPs can be functionally divided into different structural subclasses (see Fig. 1) that include: (i) the phosphonylmethoxyethyl (PME) derivatives (*e.g.* PMEA (adefovir)); (ii) the phosphonylmethoxypropyl (PMP) derivatives (*e.g.* (*R*)PMPA (tenofovir) and (*S*)FPMPA); and (iii) the hydroxyphosphonylmethoxypropyl (HPMP) derivatives (*e.g.* (*S*)HPMPA and (*S*)HPMPC (cidofovir)) (1–5). Analogs of each subclass are endowed with a characteristic and specific antiviral activity spectrum (6). For example, the PME-purine derivatives are active against several DNA viruses (*e.g.* herpesviruses, poxviruses, and hepatitis B virus) and retroviruses (*e.g.* HIV-1), whereas the PMP-purine derivatives display antiviral activity against retroviruses and hepatitis B virus only. The HPMP-purine derivatives are active against a broad variety of DNA viruses (*e.g.* herpesviruses, poxviruses, and adenoviruses), whereas the cytosine derivative (*S*)HPMPC represents the sole HPMP-pyrimidine derivative that shows selective activity against cytomegalovirus and poxviruses. Interestingly, the PME- and PMP-pyrimidine derivatives do not exhibit antiviral activity. Thus, minor structural modifications in the side chain and also the identity of the base have a marked impact on the ANP antiviral activity spectrum. All of the ANPs described above are metabolized to a diphosphate form in the cell and act as competitive inhibitors (alternative substrates) of the virus-encoded DNA polymerase (4, 7–11). The ANP-diphosphate binds to the active site of the viral polymerase and competes with the corresponding natural nucleotide (*e.g.* dATP for (*S*)HPMPA, PMEA, (*S*)FPMPA and (*R*)PMPA, and dCTP for (*S*)HPMPC) for subsequent incorporation into the growing DNA chain.

Recently, a new structural subclass of ANP, the acyclic phosphonylmethoxyethoxy- and phosphonylmethoxypropoxydiaminopyrimidines (designated PMEO- and PMPO-DAPym) derivatives, was identified (12–15). These ANPs differ from the other subclasses by the presence of an aliphatic alkyloxy linker bound to the C-6 of a 2,4-diaminopyrimidine base through an ether bond instead of the traditional alkyl linker bond to the N-1 of a pyrimidine or the N-9 of a purine (Figs. 1 and 2). Interestingly, and in contrast to the PME- and PMP-pyrimidines, the PMEO- and PMPO-pyrimidine ANP derivatives exhibit pronounced activity against both retroviruses and hepatitis B virus (16). Of further interest, these analogs display an antiviral activity spectrum that is similar to the PME- and PMP-purines. Therefore, it was speculated that there was structural similarity between the 2,6-diaminopurine (DAP) PME-derivative (PMEDAP) and the PMEO-DAPym derivatives (12). This

* This work was supported, in whole or in part, by National Institutes of Health Grant R01 AI081571 (to N. S.-C.). This work was also supported by KU Leuven Grant GOA Krediet 05/19 (to J. B.).

[1] To whom correspondence should be addressed: Rega Institute for Medical Research, Minderbroedersstraat 10, Leuven B-3000, Belgium. Tel.: 32-16-337-367; Fax: 32-16-337-340; E-mail: jan.balzarini@rega.kuleuven.be.

[2] The abbreviations used are: ANP, acyclic nucleoside phosphonate; PME, phosphonylmethoxyethyl; PMP, phosphonylmethoxypropyl; HPMP, hydroxyphosphonylmethoxypropyl; PMEO-DAPym, phosphonylmethoxyethoxydiaminopyrimidine; HIV-1, human immunodeficiency virus, type 1; RT, reverse transcriptase; T/P, template/primer; WT, wild type; TAM, thymidine analog mutation; RT, reverse transcriptase; (*R*)PMPA, phosphonylmethoxypropyl adenine; pp, diphosphate; (*S*)FPMPA, fluorophosphonylmethoxypropyl adenine; DAP, diaminopurine; PMEDAP, phosphorylmethoxyethyl diaminopurine.

Downloaded from www.jbc.org at KU Leuven - Biomedical Library, on April 19, 2010

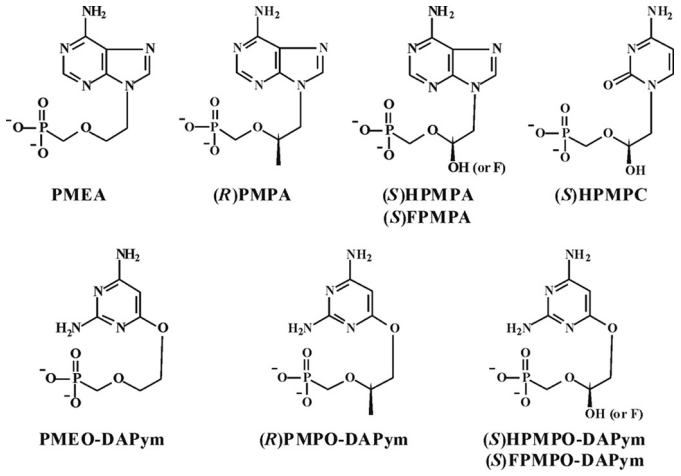

FIGURE 1. **Structures of PME (PMEA), PMP ((*R*)PMPA), and HPMP ((*S*)HPMPA, (*S*)FPMPA, and (*S*)HPMPC) ANP derivatives and the corresponding PMEO-, (*R*)PMPO-, (*S*)HPMPO-, and (*S*)FPMPO-diaminopyrimidines (DAPym).**

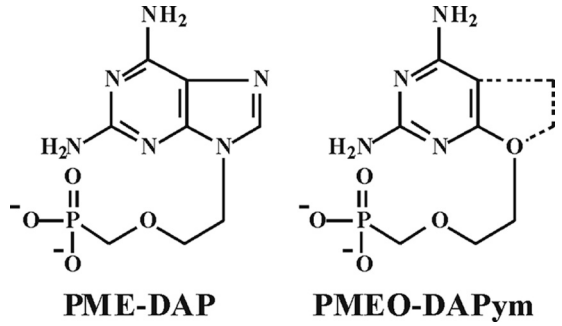

FIGURE 2. **Structural similarity between the PME-diaminopurine (DAP) derivative and PMEO-DAPym.**

was supported by molecular modeling and superimposition of their optimized three-dimensional structures, which demonstrated that the 2,4-diamino-substituted pyrimidine could be regarded as an open-ring analog of the purine system in the 2,6-diaminopurine ANPs (Fig. 2) (16).

In this study, we have analyzed the molecular interactions between PMEO-DAPym diphosphate (PMEO-DAPym-pp) and the active site of HIV-1 reverse transcriptase (RT, EC 2.7.7.49) using both steady-state and pre-steady-state kinetic analyses. The *in vitro* activity of PMEO-DAPym-pp against wild-type (WT) and drug-resistant recombinant purified HIV-1 RT was also compared with the PME-purine (*e.g.* PMEA) and PMP-purine (*e.g.* (*R*)PMPA) analogs. Importantly, we show for the first time that the acyclic pyrimidine nucleoside phosphonate derivative PMEO-DAPym-pp is incorporated into the growing DNA chain by HIV-1 RT as a purine nucleotide analog but not as a pyrimidine nucleotide analog. Therefore, PMEO-pyrimidine derivatives successfully mislead the viral DNA polymerase and act as purine nucleotide mimetics. Also, we obtained kinetic evidence that PMEO-DAPym may have a therapeutic edge over (*R*)PMPA (tenofovir) in terms of its level of phenotypic drug resistance. The identification of such modified pyrimidine analogs opens new perspectives for developing novel types of such ambiguous pyrimidine nucleosides or nucleotides with antiviral or antimetabolic potential.

EXPERIMENTAL PROCEDURES

Reagents—The WT HIV-1 RT used in the steady-state kinetic experiments that utilized homopolymeric template/primers (T/Ps) was derived from an HIV-1 (SF2 strain) *pol* gene fragment coding for the RT (Pro^{156}–Leu^{715}). The stock solution was 0.36 mg/ml. The WT, K65R, K70E, M184V, M41L/L210W/T215Y (TAM41), and D67N/K70R/T215F/K219Q (TAM67) HIV-1 RTs used in the steady-state and pre-steady-state kinetic experiments that utilized heteropolymeric T/Ps were purified as described previously (17, 18). The protein concentration of these enzymes was determined spectrophotometrically at 280 nm using an extinction coefficient (ϵ_{280}) of 260,450 M^{-1} cm^{-1} and by Bradford protein assays (Sigma-Aldrich). The RNA- and DNA-dependent DNA polymerase activities of the purified WT and mutant enzymes were essentially identical (data not shown). (*R*)PMPA diphosphate ((*R*)PMPA-pp) and PMEA diphosphate (PMEA-pp) were purchased from Moravek Biohemicals (Brea, CA). PMEO-DAPym-pp was synthesized and provided by A. Holý (Prague, Czech Republic). ATP, dNTPs, and ddNTPs were purchased from Amersham Biosciences, and [γ-^{32}P]ATP was acquired from PerkinElmer Life Sciences. RNA and DNA heteropolymeric oligonucleotides were synthesized by IDT (Coralville, IA). The templates poly(rC), poly(rA), poly(rI), and poly(rU) as well as the primers oligo(dG)$_{12-18}$, oligo(dT)$_{12-18}$, oligo(dC)$_{12-18}$, and oligo(dA)$_{12-18}$ were from Amersham Biosciences. The hompolymeric T/P substrates poly(rC)/oligo(dG), poly(rA)/oligo(dT), poly(rI)/oligo(dC), and poly(rU)/oligo(dA) were prepared by mixing 0.15 mM template with an equal volume of 0.0375 mM primer.

Steady-state Assays Using Homopolymeric T/Ps—Reactions (50 μl in volume) were carried out in a 50 mM Tris-HC1 (pH 7.8) buffer that contained 5 mM dithiothreitol, 300 mM glutathione, 0.5 mM EDTA, 150 mM KC1, 5 mM $MgC1_2$, or 5 mM $MnCl_2$, 1.25 μg of bovine serum albumin, 0.06% Triton X-100, an appropriate concentration of [^{3}H]dTTP, [^{3}H]dGTP, [^{3}H]dCTP, or [^{3}H]dATP (2 μCi/assay), varying concentrations of ANP analog, and a fixed concentration of poly(rA)/oligo(dT) (0.015 mM), poly(rC)/oligo(dG) (0.1 mM), poly(rI)/oligo(dC) (0.015 mM), or poly(rU)/oligo(dA) (0.015 mM). Reactions were initiated by the addition of 1 μl of RT and were incubated for 15 min at 37 °C. Reactions were then terminated by the addition of 100 μl of 150 μg/ml calf thymus DNA, 2 ml of 0.1 M $Na_4P_2O_7$ (in 1 M HCl), and 2 ml of 10% (v/v) trichloroacetic acid. The solutions were kept on ice for 30 min after which the acid-insoluble material was washed and analyzed for radioactivity. For 50% inhibitory concentration (IC_{50}) determinations, fixed concentrations of 1.25 μM [^{3}H]dTTP, 2.5 μM [^{3}H]dGTP, 1.75 μM [^{3}H]dATP, or 2.5 μM [^{3}H]dCTP were used. For the K_i determinations with respect to the natural substrates, a fixed concentration of T/P was used (as indicated above). For the K_i determinations with respect to T/P, varying concentrations of the T/P were used in the presence of a fixed concentration of 1.25 μM [^{3}H]dTTP, 2.5 μM [^{3}H]dGTP, 1.75 μM [^{3}H]dATP, or 2.5 μM [^{3}H]dCTP. The steady-state kinetic constants K_i and K_m were determined by linear regression using double-reciprocal Lineweaver-Burke plots.

Steady-state Assays Using Heteropolymeric T/P—The ability of PMEO-DAPym-pp to inhibit HIV-1 RT DNA synthesis was also evaluated using heteropolymeric DNA/DNA and RNA/

Downloaded from www.jbc.org at KU Leuven - Biomedical Library, on April 19, 2010

TABLE 1
Inhibition of HIV-1 RT-mediated DNA synthesis by PMEO-DAPym-pp and other nucleoside analogs on homopolymeric T/Ps

	IC_{50}[a]							
	Poly(rC)/oligo(dG) [^{3}H]dGTP		Poly(rU)/oligo(dA) [^{3}H]dATP		Poly(rA)/oligo(dT) [^{3}H]dTTP		Poly(rI)/oligo(dC) [^{3}H]dCTP	
	$MgCl_2$	$MnCl_2$	$MgCl_2$	$MnCl_2$	$MgCl_2$	$MnCl_2$	$MgCl_2$	$MnCl_2$
	μM							
PMEO-DAPym-pp	>200	16 ± 3.3	ND[b]	0.26 ± 0.10	>200	>200	>200	>200
PMEA-pp	>100	75 ± 21	ND	0.12 ± 0.06	>100	>100	>100	>100
ddATP	>100	72 ± 13	ND	0.23 ± 0.17	>100	>100	>100	>100
ddTTP	>100	>100	ND	>100	0.053 ± 0.011	0.072 ± 0.001	>100	>100
AZTTP	>100	>100	ND	67 ± 7	0.024 ± 0.020	0.006 ± 0.004	>100	59 ± 7

[a] The 50% inhibitory concentration (μM) required to inhibit the enzyme reaction by 50%. The concentration of $MgCl_2$ or $MnCl_2$ in the reaction mixture was 5 mM. Data are the mean ± S.D. of two to three independent determinations.
[b] ND, not detectable.

DNA T/Ps. Briefly, reactions were carried out in 50 mM Tris (pH 7.5), 50 mM KCl, 10 mM $MgCl_2$ containing 20 nM T/P, 0.5 μM each dNTP, and various concentrations of PMEO-DAPym-pp (0–40 μM). The sequences of the T/P substrates are provided in Fig. 4, and the DNA primers were 5′-radiolabeled with [γ-^{32}P]ATP as described previously (19). Reactions were initiated by the addition of 200 nM WT RT, incubated for 10 min at 37 °C, and then quenched using 20 μl of gel-loading buffer (98% deionized formamide containing 1 mg/ml each of bromphenol blue and xylene cyanol). Control reactions included the addition of either (*R*)PMPA-pp or PMEA-pp. Samples were then denatured at 95 °C for 10 min, and polymerization products were separated from substrates by denaturing gel electrophoresis using 14% acrylamide containing 7 M urea. Gels were analyzed using phosphorimaging with a GS525 Molecular Imager and Quantity One Software (Bio-Rad). The concentration of ANP-diphosphate required to inhibit the formation of final product by 50% was calculated using non-linear regression from at least three independent experiments. The amount of final product was quantified by densitometric analysis using Quantity One Software.

Pre-steady-state Assays—A rapid quench instrument (Kintek RQF-3 instrument, Kintek Corp., Clarence, PA) was used for pre-steady-state experiments with reaction times ranging from 20 ms to 60 s. The typical experiment was performed at 37 °C in 50 mM Tris-HCl (pH 7.5) containing 50 mM KCl, 10 mM $MgCl_2$, and varying concentrations of nucleotide. All concentrations reported refer to the final concentrations after mixing. HIV-1 RT (200 nM) was preincubated with 20 nM T/P substrate, prior to rapid mixing with nucleotide and divalent metal ions to initiate the reaction that was quenched with 0.5 M EDTA. The sequences of the template and 5′-radiolabeled primer were 5′-CTCAGACCCTTTTAGTCAGAATGGAAATTCTCTAGCAGTGGCGCCCGAACAGGGACA-3′ and 5′-TCGGGCGCCACTGCTAGAGA-3′, respectively. The quenched samples were then mixed with an equal volume of gel loading buffer, and products were separated from substrates as described above. The disappearance of substrate (20-mer) and the formation of product (21-mer) were quantified using a Bio-Rad GS525 Molecular Imager (Bio-Rad). Data were fitted by non-linear regression with Sigma Plot software (Systat Software, Inc., San Jose, CA) using the appropriate equations (20). The apparent burst rate constant (k_{obs}) for each particular concentration of dNTP was determined by fitting the time courses for the formation of product (21-mer) using the following equation: $[21\text{-mer}] = A[1 - \exp(-k_{obs}t)]$, where A represents the burst amplitude. The turnover number (k_{pol}) and apparent dissociation constant for dNTP (K_d) were then obtained by plotting the apparent catalytic rates (k_{obs}) against dNTP concentrations and fitting the data with the following hyperbolic equation: $k_{obs} = (k_{pol}[\text{dNTP}])/([\text{dNTP}] + K_d)$. Catalytic efficiency was calculated as the ratio of turnover number over dissociation constant ($[k_{pol}/K_d]$). Selectivity for natural dNTP *versus* ANP was calculated as the ratio of catalytic efficiency of dNTP over that of ANP ($[(k_{pol}/K_d)^{dNTP}/(k_{pol}/K_d)^{ANP}]$). Resistance was calculated as the ratio of selectivity of the mutant over that of WT ($[(\text{selectivity})^{Mutant}/(\text{selectivity})^{WT}]$).

Excision Assays—A 26-nucleotide DNA primer (P; 5′-CCTGTTCGGGCGCCACTGCTAGAGAT-3′) was 5′-radiolabeled with [γ-^{32}P]ATP and chain-terminated with either PMEO-DAPym-pp, (*R*)PMPA-pp, or PMEA-pp as reported previously (19). This chain-terminated primer was then annealed to a DNA template (5′-CTCAGACCCTTTTAGTCAGAATGGAAATTCTCTAGCAGTGGCGCCCGAACAGGGACA-3′). ATP-mediated excision assays were carried out by first incubating 20 nM T/P with 3 mM ATP, 10 mM $MgCl_2$, 1 μM dATP, and 10 μM ddGTP in a buffer containing 50 mM Tris-HCl (pH 7.5) and 50 mM KCl. Reactions were initiated by the addition of 200 nM WT or mutant RT. Aliquots were removed at defined times, quenched with sample loading buffer, and denatured at 95 °C for 10 min, and then the product was resolved from substrate by denaturing polyacrylamide gel electrophoresis and analyzed, as described above. Dead-end complex formation was evaluated using the same assay set-up described above. However, the concentration of the next correct dNTP (*i.e.* dATP) was varied from 0 to 100 μM, and reactions were quenched after 60 min.

Molecular Modeling—Molecular models were constructed using the x-ray crystallographic coordinates for the RT·T/P·(*R*)PMPA-pp ternary complex (21) (PDB, 1T05). PMEO-DAPym-pp was docked into the DNA polymerization active site, and energy minimization experiments were carried out using Molecular Operating Environment (Chemical Computing Group, Montreal, Quebec, Canada). Charges were calculated using the Gasteiger method, and iterative minimizations were carried out using the AMBER 99 forcefield until the energy difference between iterations was <0.0001 kcal/mol per Å.

Downloaded from www.jbc.org at KU Leuven - Biomedical Library, on April 19, 2010

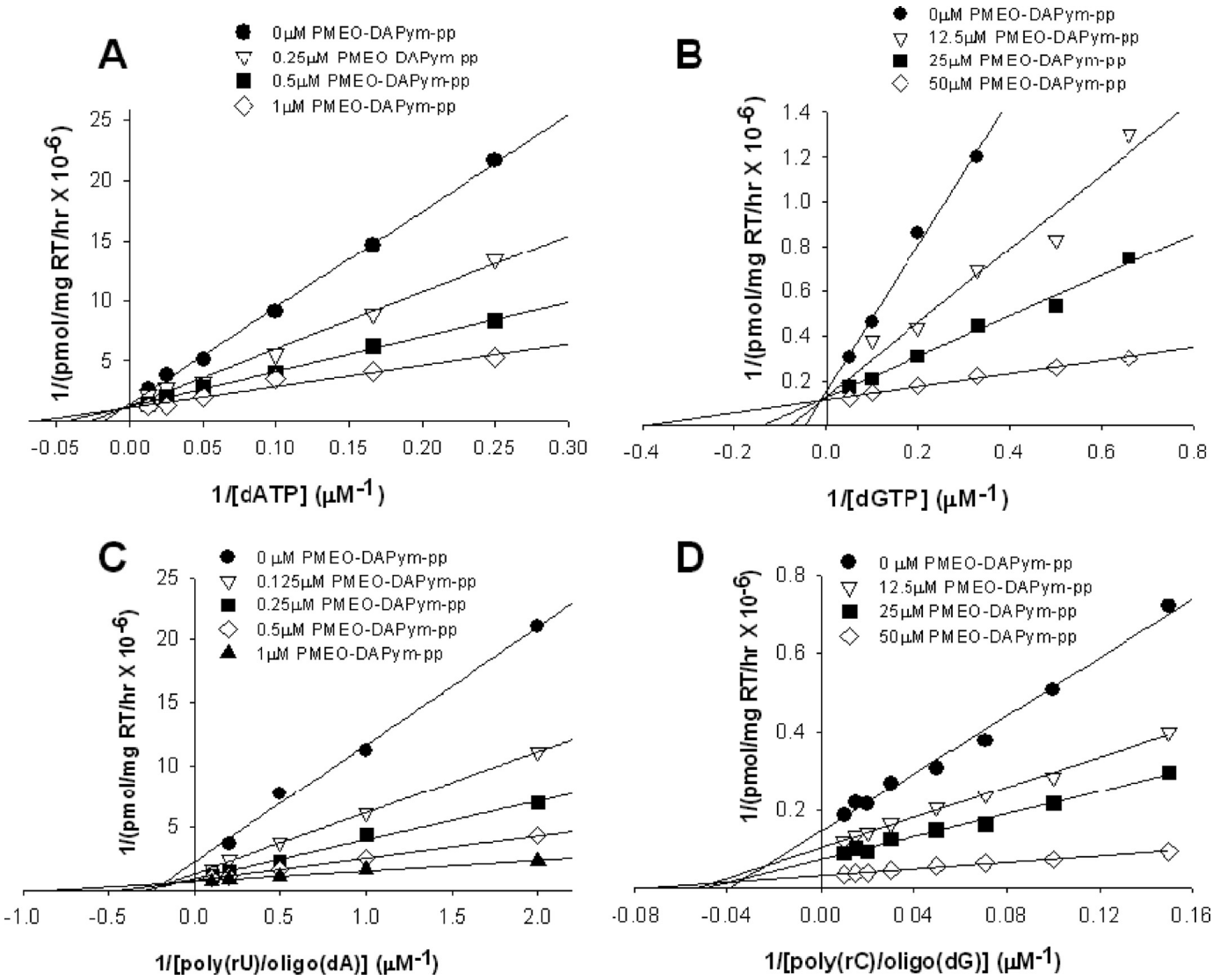

FIGURE 3. **Double-reciprocal plots for HIV-1 RT inhibition by PMEO-DAPym-pp using poly(rU)/oligo(dA) and $MnCl_2$-dATP or poly(rC)/oligo(dG) and $MnCl_2$-dGTP as substrates.** The assay conditions are described under "Experimental Procedures." PMEO-DAPym-pp was determined to be a competitive inhibitor of dATP (*A*) and dGTP (*B*) binding and a linear mixed-type inhibitor of poly(rU)/oligo(dA) (*C*) or poly(rC)/oligo(dG) (*D*) binding. The K_i values determined from these experiments are provided in Table 2.

TABLE 2

K_m- and K_i-values for PMEO-DAPym-pp and PMEA-pp against HIV-1 RT using homopolymeric T/Ps

The K_m and K_i values (μM) were calculated from the kinetic data in Fig. 3 using linear regression analysis. Data are the mean ± S.D. of two to three independent experiments.

Inhibitor	Competing entity							
	Poly(rU)/oligo(dA)		dATP		Poly(rC)/oligo(dG)		dGTP	
	K_m	K_i	K_m	K_i	K_m	K_i	K_m	K_i
				μM				
PMEO-DAPym-pp	1.2 ± 0.1	0.41 ± 0.10	16 ± 5	0.29 ± 0.22	17 ± 10	12 ± 2.2	2.7 ± 0.5	5.8 ± 1.2
PMEA-pp	1.2 ± 0.4	0.12 ± 0.05	10 ± 2	0.10 ± 0.06	17 ± 10	46 ± 1.0	3.0 ± 0.7	39 ± 5.7

RESULTS AND DISCUSSION

Inhibition of HIV-1 RT-mediated DNA Synthesis by PMEO-DAPym-pp in the Presence of Homopolymeric T/Ps—The ability of PMEO-DAPym-pp to inhibit HIV-1 RT-mediated DNA synthesis was first evaluated using four different homopolymeric T/Ps (Table 1). PMEA-pp and the 2′,3′-dideoxynucleotide derivatives ddATP, ddTTP, and AZT-TP were included as controls in these experiments. Reactions were carried out using either $MgCl_2$ or $MnCl_2$ as the divalent metal ion. In general, $MgCl_2$-mediated DNA polymerization reactions proceeded 10- to 100-fold more efficiently than $MnCl_2$-mediated reactions when poly(rC)/oligo(dG), poly(rA)/oligo(dT), or poly(rI)/oligo (dC) were used as the T/P substrate. By contrast, efficient DNA synthesis on the poly(rU)/oligo(dA) T/P was only observed when $MnCl_2$ was used as the divalent metal ion (data not shown). PMEO-DAPym-pp showed pronounced submicromo-

Downloaded from www.jbc.org at KU Leuven - Biomedical Library, on April 19, 2010

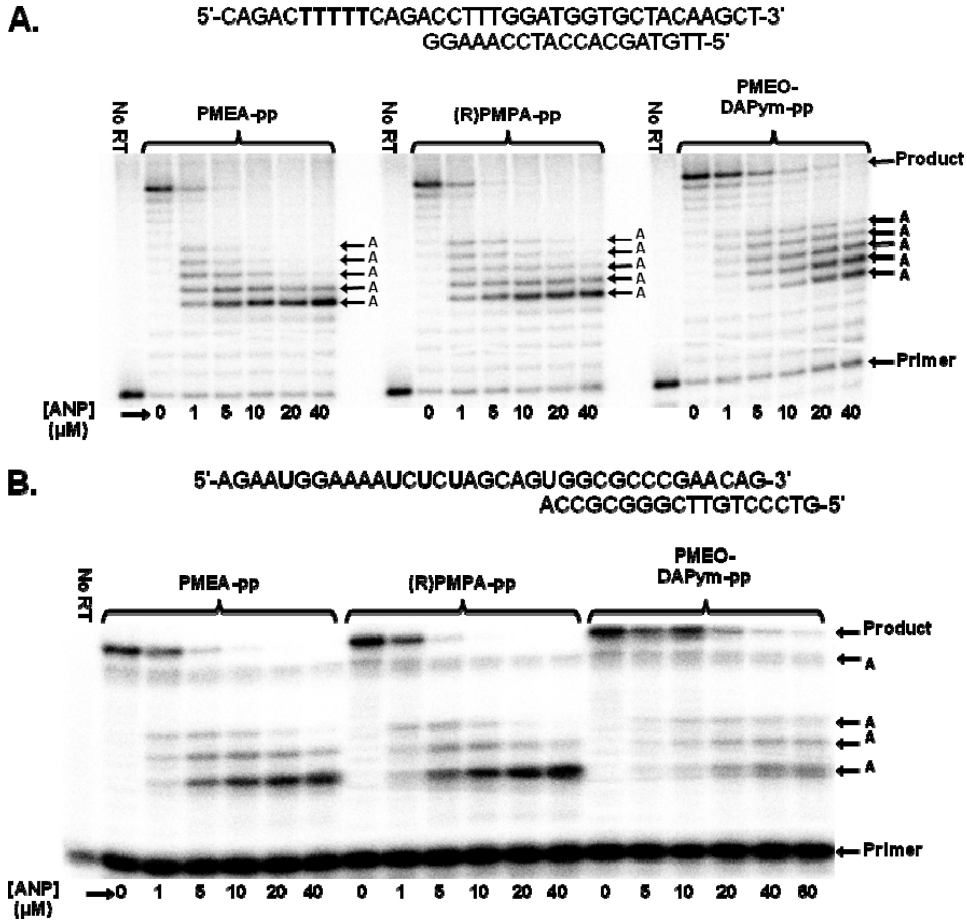

FIGURE 4. **Incorporation of PMEO-DAPym-pp as an adenosine analog by WT HIV-1 RT in DNA/DNA (*A*) or RNA/DNA (*B*) T/P.** The sequences of the DNA/DNA and RNA/DNA T/P are indicated above each autoradiogram.

lar inhibitory activity (IC_{50} = 0.26 μM), that was similar to PMEA-pp (IC_{50} = 0.12 μM) or ddATP (IC_{50} = 0.23 μM), when poly(rU)/oligo(dA) and $MnCl_2$-dATP were used as substrates. By contrast, 385- and 257-fold higher concentrations of ddTTP and AZT-TP, respectively, were required to inhibit DNA synthesis using the same substrates (Table 1). Interestingly, whereas PMEO-DAPym-pp did not inhibit reactions on the poly(rA)/oligo(dT) or poly(rI)/oligo(dC) T/P substrates at 200 μM, the compound was found to exert modest inhibition (IC_{50} = 16 μM) when poly(rC)/oligo(dG) and $MnCl_2$-dGTP were used as substrates. By contrast, PMEA-pp and ddATP did not show pronounced inhibitory activity (IC_{50} as high as 72–75 μM) under similar assay conditions (Table 1). Interestingly, no inhibition of DNA synthesis was observed at concentrations of 100 μM PMEO-DAPym-pp when $MnCl_2$ was replaced by $MgCl_2$. Additional studies demonstrated that PMEO-DAPym-pp acted as a competitive inhibitor of $MnCl_2$-[^{3}H]dATP or $MnCl_2$-[3H]dGTP binding, and as a linear mixed-type inhibitor of poly(rU)/oligo(dA) or poly(rC)/oligo(dG) binding (Fig. 3). The Michaelis-Menten constants, K_m and K_i, determined from these experiments are provided in Table 2. Taken together, these data demonstrate that HIV-1 RT recognizes and incorporates PMEO-DAPym-pp as an adenine nucleotide derivative. The fact that PMEO-DAPym-pp was also weakly incorporated by HIV-1 RT into the poly(rC)/oligo(dG) T/P substrates when $MnCl_2$ was used as the divalent metal ion suggests that this nucleotide might also base pair with cytosine. Alternatively, it is well known that nucleotide misincorporation is more readily facilitated by $MnCl_2$ in comparison with $MgCl_2$, because $MnCl_2$ can partially compensate for the rate-limiting chemistry step that governs misincorporation reactions (22). The fact that PMEO-DAPym-pp incorporation is not observed opposite cytosine in the more physiologically relevant heteropolymeric T/P substrate might also suggest that this result is an artifact inherent to the homopolymeric T/P substrate.

Inhibition of HIV-1 RT-mediated DNA Synthesis by PMEO-DAPym-pp in the Presence of Heteropolymeric T/Ps—We next examined the ability of PMEO-DAPym-pp to inhibit HIV-1 RT-mediated DNA polymerization on heteropolymeric DNA/DNA and RNA/DNA T/Ps with $MgCl_2$ as the divalent metal cation (Fig. 4). In these experiments, (*R*)PMPA-pp and PMEA-pp were included as controls. Consistent with the studies described above, we found that HIV-1 RT recognized PMEO-DAPym-pp as a purine but not a pyrimidine nucleotide analog and incorporated it opposite to thymine in the DNA template or uracil in the RNA template. As expected, its incorporation resulted in chain termination of DNA synthesis. The concentration of PMEO-DAPym-pp required to inhibit HIV-1 RT-catalyzed DNA synthesis by 50% (IC_{50}) was calculated to be 3.5 μM and 15 μM on the DNA/DNA and RNA/DNA template/primer substrates, respectively. By comparison, the IC_{50} values for (*R*)PMPA-pp and PMEA-pp were calculated to be 0.79 μM and 0.78 μM for the DNA/DNA, and 1.83 μM and 1.21 μM for the RNA/DNA T/P substrates, respectively. In these assays, PMEO-DAPym-pp was not incorporated opposite to the alternative pyrimidine cytosine, even when $MnCl_2$ was used as the divalent metal ion (data not shown).

Pre-steady-state Incorporation of PMEO-DAPym-pp by WT, K65R, K70E, and M184V HIV-1 RT—Pre-steady-state kinetic analyses were carried out to elucidate, in detail, the interactions between PMEO-DAPym-pp and the polymerase active site of HIV-1 RT (Table 3). Because PMEO-DAPym-pp behaves as an adenine nucleotide analog, we again included (*R*)PMPA-pp and PMEA-pp as controls. In addition, we examined the activity of PMEO-DAPym-pp against RTs containing the K65R and K70E mutations that are associated with (*R*)PMPA and PMEA resistance, respectively (23, 24). In addition, we investigated the activity of PMEO-DAPym-pp against M184V containing HIV-1 RT, because this mutation has been reported to confer

Downloaded from www.jbc.org at KU Leuven - Biomedical Library, on April 19, 2010

TABLE 3
Pre-steady state kinetic incorporation values for WT and drug-resistant HIV-1 RT

	dATP			ANP			Selectivity[a]	Resistance[b]
	k_{pol}	K_d	k_{pol}/K_d	k_{pol}	K_d	k_{pol}/K_d		
	s^{-1}	μM	$\mu M^{-1}\ s^{-1}$	s^{-1}	μM	$\mu M^{-1}\ s^{-1}$		
PMEO-DAPym-pp								
WT	24.4 ± 3.9[c]	3.2 ± 1.2	7.6	1.1 ± 0.3	2.3 ± 1.1	0.49	15.5	
K65R	12.6 ± 1.9	3.2 ± 0.7	4.0	0.21 ± 0.04	3.5 ± 2.1	0.06	65.8	4.2
K70E	18.0 ± 2.8	3.3 ± 0.9	5.5	0.18 ± 0.01	2.3 ± 0.6	0.08	69.3	4.5
M184V	14.8 ± 6.4	2.5 ± 0.8	5.9	1.2 ± 0.08	4.3 ± 0.2	0.27	21.7	1.4
(*R*)PMPA-pp								
WT	24.4 ± 3.9	3.2 ± 1.2	7.6	6.16 ± 1.0	4.3 ± 1.0	1.44	5.3	
K65R	12.6 ± 1.9	3.2 ± 0.7	4.0	0.45 ± 0.06	7.3 ± 2.7	0.06	65.8	12.4
K70E	18.0 ± 2.8	3.3 ± 0.9	5.5	2.1 ± 0.1	5.1 ± 1.5	0.41	13.5	2.5
M184V	14.8 ± 6.4	2.5 ± 0.8	5.9	2.0 ± 0.9	2.6 ± 0.3	0.76	7.8	1.5
PMEA-pp								
WT	24.4 ± 3.9	3.2 ± 1.2	7.6	5.1 ± 1.3	4.0 ± 1.5	1.26	6.0	
K65R	12.6 ± 1.9	3.2 ± 0.7	4.0	0.52 ± 0.28	4.2 ± 1.8	0.12	32.9	5.5
K70E	18.0 ± 2.8	3.3 ± 0.9	5.5	2.5 ± 0.5	4.3 ± 1.4	0.59	9.39	1.6
M184V	14.8 ± 6.4	2.5 ± 0.8	5.9	1.95 ± 0.6	3.4 ± 1.3	0.57	10.3	1.7

[a] Selectivity is $(k_{pol}/K_d)^{dNTP}/(k_{pol}/K_d)^{ANP}$.
[b] Resistance (*n*-fold) is selectivity^{mutant}/selectivity^{WT}.
[c] Values represent mean ± S.D. of three independent experiments.

TABLE 4
Excision rates and dead-end complex formation by WT and mutant RT

	Excision rate[a]			IC_{50} for DEC formation[b]		
	(*R*)PMPA	PMEA	PMEO-DAPym	(*R*)PMPA	PMEA	PMEO-DAPym
	min^{-1}	min^{-1}	min^{-1}	μM	μM	μM
WT	0.024 ± 0.00	0.014 ± 0.00	0.025 ± 0.01	30.1 ± 6.5	14.7 ± 2.7	14.6 ± 1.8
TAM67[c]	0.088 ± 0.02 (3.7)[d]	0.043 ± 0.01 (3.1)	0.080 ± 0.01 (3.2)	79.0 ± 4.5	65.9 ± 1.6	67.4 ± 4.6
TAM41[e]	0.086 ± 0.02 (3.6)	0.030 ± 0.01 (2.1)	0.065 ± 0.01 (2.6)	78.3 ± 5.4	50.0 ± 9.0	55.6 ± 7.5

[a] Values represent mean ± S.D. from two independent experiments.
[b] Values represent mean ± S.D. from three independent experiments.
[c] TAM67: D67N/K70R/T215F/K219Q.
[d] Values in parentheses indicate -fold change compared to WT RT.
[e] TAM41: M41L/L210W/T215Y.

hypersusceptibility to (*R*)PMPA-pp in transient kinetic analyses (29). The results (Table 3) show that the catalytic efficiency of incorporation (k_{pol}/K_d) of PMEO-DAPym-pp for WT HIV-1 RT is ~2- to 3-fold less than the k_{pol}/K_d values determined for PMEA-pp or (*R*)PMPA-pp. This decrease in the k_{pol}/K_d value for PMEO-DAPym-pp (relative to PMEA-pp and (*R*)PMPA-pp) is driven predominantly by a slower rate of nucleotide analog incorporation (k_{pol}) and not by a diminished binding affinity (K_d) for the DNA polymerase active site of RT. As reported previously, the catalytic efficiency of incorporation of (*R*)PMPA-pp is decreased 12.4- and 2.5-fold by the K65R and K70E mutations in RT (17, 18). Consistent with previously published cross-resistance data (23, 24), both the K65R and K70E mutations in HIV-1 RT also conferred resistance to PMEA-pp. Similar to (*R*)PMPA-pp, this resistance was driven primarily by a selective decrease in the rate of PMEA-pp incorporation (k_{pol}) and not by a decrease in the nucleotide binding affinity (K_d). Both the K65R and K70E mutations in RT also conferred resistance to PMEO-DAPym-pp via a similar mechanism (*i.e.* selective decrease in k_{pol}). However, PMEO-DAPym-pp displayed better incorporation activity against K65R RT than (*R*)PMPA-pp. In this regard, a previous study reported that PMEO-DAPym exhibited better antiviral activity (lower levels of phenotypic drug resistance) against a panel of clinical virus isolates that contained multiple drug resistance mutations, including K65R, than did either PMEA or (*R*)PMPA (15). Furthermore, these data also highlight that subtle changes in the side chains and identity of the base part have a marked impact on the ANP antiviral activity spectrum. Finally, our data also show that HIV-1 RT containing M184V remains sensitive to inhibition by PMEO-DAPym-pp, PMEA-pp, and (*R*)PMPA-pp. In this regard, Deval *et al.* previously reported that M184V HIV-1 RT showed increased susceptibility to (*R*)PMPA-pp in pre-steady-state kinetic assays (29). In this study, the (*R*)PMPA-pp hypersusceptibility was primarily driven by a decreased catalytic efficiency for dATP (but not (*R*)PMPA-pp) incorporation by M184V HIV-1 RT. By contrast, we did not observe (*R*)PMPA-pp hypersusceptibility by M184V HIV-1 RT: the catalytic efficiency of dATP incorporation (k_{pol}/K_d) by M184V RT was not significantly decreased relative to the WT enzyme (Table 4). The different results obtained in these two studies might be due to sequence-specific differences resulting from the different T/P substrates used.

ATP-mediated Excision of PMEO-DAPym by WT and Mutant HIV-1 RT—HIV-1 RT has the intrinsic ability to rescue DNA synthesis from a blocked primer by ATP-mediated phosphorolytic excision of the DNA chain-terminating nucleotide (25). This ATP-mediated excision activity of HIV-1 RT is selectively increased by thymidine analog mutations (TAMs) (26, 27) but can be diminished by other mutations, including K65R and K70E (17, 18). Accordingly, we next investigated the ability of WT, K65R, K70E, and TAM-

Downloaded from www.jbc.org at KU Leuven - Biomedical Library, on April 19, 2010

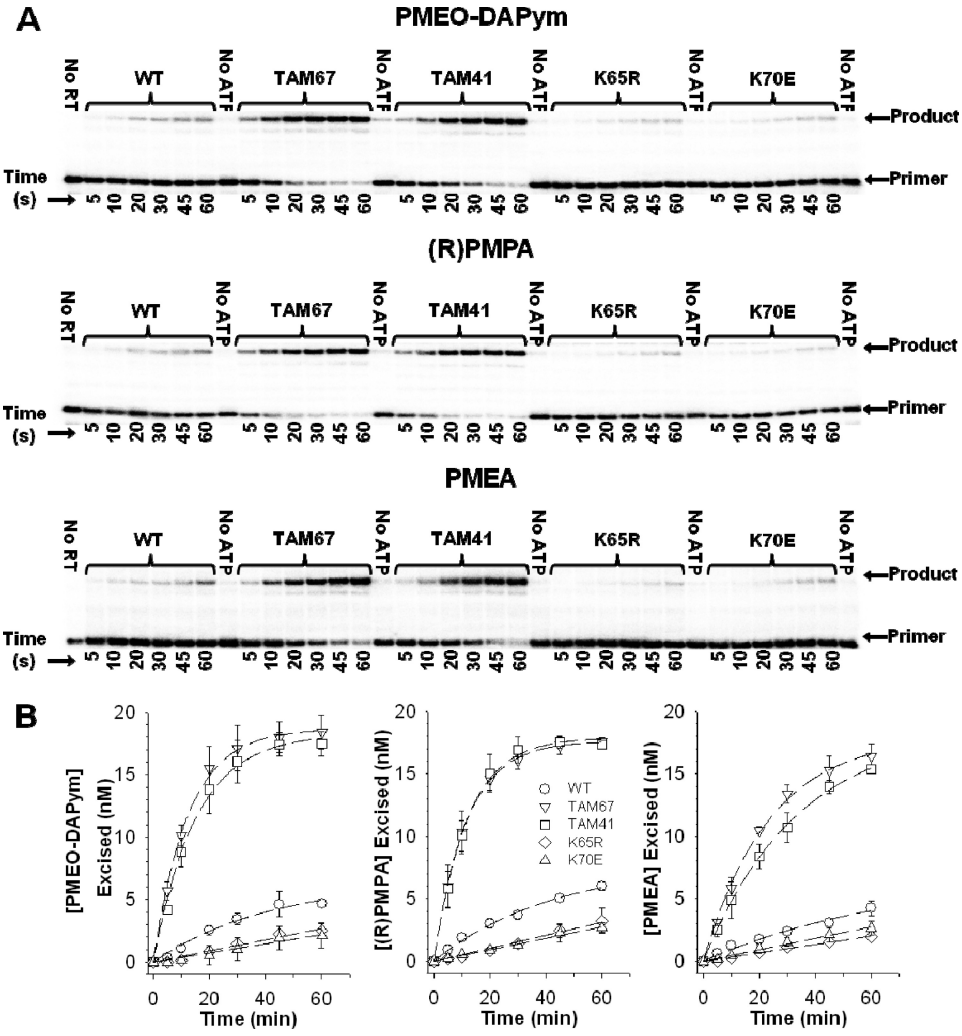

FIGURE 5. **Autoradiograms (*A*) and rates (*B*) for ATP-mediated excision of PMEO-DAPym, (*R*)PMPA, and PMEA by WT and mutant HIV-1 RT.** For *B*, data represent the mean ± S.D. of two independent experiments.

containing RT to excise PMEO-DAPym from a DNA chain-terminated T/P. Two RT enzymes that contained different patterns of TAMs (*e.g.* M41L/L210W/T215Y (TAM41) and D67N/K70R/T215F/K219Q (TAM67)) were included in this study. In addition, (*R*)PMPA- and PMEA-chain-terminated DNAs were included as controls. The results (Fig. 5 and Table 4) demonstrate that, in comparison with the WT enzyme, both TAM41 and TAM67 HIV-1 RT exhibited increased capacities to excise all three ANPs. However, the excision of PMEA and PMEO-DAPym by TAM41 RT occurred less efficiently than that of (*R*)PMPA. In contrast to the RTs containing TAMs, the mutant K70E and K65R RT enzymes exhibited poor excision activity that was independent of the DNA chain-terminating nucleotide analog. Previous studies have shown that the next complementary nucleotide can inhibit ATP-mediated chain terminator removal (28). To determine the magnitude and nature of this inhibition against PMEO-DAPymp, PMEA, and (*R*)PMPA, we determined the 50% inhibitory concentrations (IC_{50}) of the next complementary nucleotide for the ATP-dependent removal of each of the acyclic nucleoside phosphonate analogs. The results (Table 4) show that the inhibitory concentrations of the next complementary dNTP were found to be somewhat higher for (*R*)PMPA compared with either PMEA and PMEO-DAPym. Taken together, these data suggest that PMEO-DAPym is a less efficient substrate for ATP-mediated excision than (*R*)PMPA. These findings may suggest that PMEO-DAPym may eventually be superior to (*R*)PMPA as an antiretroviral drug in respect of phenotypic drug resistance levels.

Molecular Modeling—A molecular model of PMEO-DAPym-pp bound at the DNA polymerase active site of HIV-1 RT was generated by docking this compound into the RT·T/P·(R)PMPA-pp structure (PDB coordinate 1T05). The model (Fig. 6*A*) shows that PMEO-DAPym-pp can reside in the DNA polymerase active site of RT without significant perturbation of its key residues (*e.g.* Lys^{65}, Arg^{72}, Asp^{110}, Tyr^{115}, Asp^{185}, Asp^{186}, and Gln^{151}). In fact, overlay of the RT·T/P·(R)PMPA-pp structure with our model suggests that the active site architecture is essentially unchanged, including the YMDD motif that is essential for catalysis (Fig. 6*B*). In addition, the model shows that the C-6 phosphonate linkage allows the pyrimidine ring in PMEO-DAPym to mimic an open incomplete purine ring that allows the canonical Watson-Crick base pairing to be maintained.

Conclusions—In the present study, we demonstrate that HIV-1 RT efficiently recognizes PMEO-DAPym-pp as a purine (*e.g.* adenine) nucleotide derivative but not as a pyrimidine nucleotide derivative. Our modeling and docking studies in HIV-1 RT confirm the similarities between PMEO-DAPym-pp and (*R*)PMPA-pp in terms of a mimetic of an incomplete purine ring (DAPym) and are in full agreement with the obtained kinetic data. This is a striking observation and the first demonstration that a pyrimidine nucleotide analog can be unambiguously recognized as an adenine nucleotide derivative for both binding and incorporation into the growing DNA chain by HIV-1 RT. Moreover, such wrongly incorporated nucleotide derivative shows a lesser efficient increase of excision from the terminated DNA chain by mutant RTs than (*R*)PMPA. Such drugs may make it more difficult to the virus to escape drug pressure and may eventually exert lower phenotypic drug resistance levels, as

Downloaded from www.jbc.org at KU Leuven - Biomedical Library, on April 19, 2010

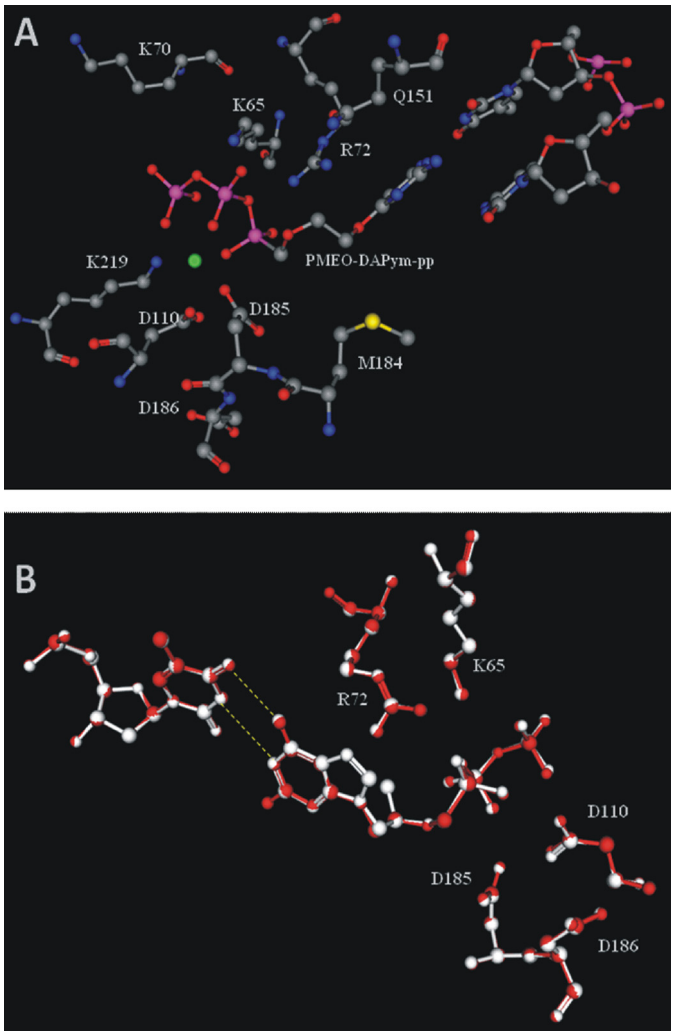

FIGURE 6. **A model of PMEO-DAPym-pp bound at the DNA polymerase active site of HIV-1 RT (*A*).** PMEO-DAPym-pp was docked into the RT·T/P·(*R*)PMPA-pp ternary structure (PDB coordinate 1T05). No significant disruption of the active site residues was observed. In *B*, an overlay of the RT·T/P·PMEO-DAPym-pp model with the RT·T/P·(*R*)PMPA-pp structure demonstrates that PMEO-DAPym-pp mimics an incomplete purine ring and allows canonical Watson-Crick base pairing.

experimentally already shown in cell culture when PMEO-DAPym is compared with (*R*)PMPA (15).

Acknowledgments—The technical assistance and secretarial assistance of Lizette van Berckelaer, Eva Tloustova, and Christiane Callebaut is greatly appreciated.

REFERENCES

1. De Clercq, E., Holý, A., Rosenberg, I., Sakuma, T., Balzarini, J., and Maudgal, P. C. (1986) *Nature* **323,** 464–467
2. De Clercq, E., Sakuma, T., Baba, M., Pauwels, R., Balzarini, J., Rosenberg, I., and Holý, A. (1987) *Antiviral Res.* **8,** 261–272
3. Pauwels, R., Balzarini, J., Schols, D., Baba, M., Desmyter, J., Rosenberg, I., Holy, A., and De Clercq, E. (1988) *Antimicrob. Agents Chemother.* **32,** 1025–1030
4. Balzarini, J., Holy, A., Jindrich, J., Dvorakova, H., Hao, Z., Snoeck, R., Herdewijn, P., Johns, D. G., and De Clercq, E. (1991) *Proc. Natl. Acad. Sci. U.S.A.* **88,** 4961–4965
5. Balzarini, J., Holy, A., Jindrich, J., Naesens, L., Snoeck, R., Schols, D., and De Clercq, E. (1993) *Antimicrob. Agents Chemother.* **37,** 332–338
6. De Clercq, E. (2007) *Biochem. Pharmacol.* **73,** 911–922
7. Mul, Y. M., van Miltenburg, R. T., De Clercq, E., and van der Vliet, P. C. (1989) *Nucleic Acids Res.* **17,** 8917–8929
8. Holý, A., Votruba, I., Merta, A., Cerný, J., Veselý, J., Vlach, J., Sedivá, K., Rosenberg, I., Otmar, M., Hrebabecký, H., Travnicek, M., Vonka, V., Snoeck, R., and De Clercq, E. (1990) *Antiviral Res.* **13,** 295–311
9. Xiong, X., Smith, J. L., Kim, C., Huang, E. S., and Chen, M. S. (1996) *Biochem. Pharmacol.* **51,** 1563–1567
10. Magee, W. C., Aldern, K. A., Hostetler, K. Y., and Evans, D. H. (2008) *Antimicrob. Agents Chemother.* **52,** 586–597
11. Xiong, X., Smith, J. L., and Chen, M. S. (1997) *Antimicrob. Agents Chemother.* **41,** 594–599
12. Balzarini, J., Pannecouque, C., De Clercq, E., Aquaro, S., Perno, C. F., Egberink, H., and Holý, A. (2002) *Antimicrob. Agents Chemother.* **46,** 2185–2193
13. Holý, A., Votruba, I., Masojídková, M., Andrei, G., Snoeck, R., Naesens, L., De Clercq, E., and Balzarini, J. (2002) *J. Med. Chem.* **45,** 1918–1929
14. Hocková, D., Holý, A., Masojídková, M., Andrei, G., Snoeck, R., De Clercq, E., and Balzarini, J. (2003) *J. Med. Chem.* **46,** 5064–5073
15. Balzarini, J., Schols, D., Van Laethem, K., De Clercq, E., Hocková, D., Masojidkova, M., and Holý, A. (2007) *J. Antimicrob. Chemother.* **59,** 80–86
16. Ying, C., Holy, A., Hocková, D., Havlas, Z., De Clercq, E., and Neyts, J. (2005) *Antimicrob. Agents Chemother.* **49,** 1177–1180
17. Sluis-Cremer, N., Sheen, C. W., Zelina, S., Torres, P. S., Parikh, U. M., and Mellors, J. W. (2007) *Antimicrob. Agents Chemother.* **51,** 48–53
18. Parikh, U. M., Zelina, S., Sluis-Cremer, N., and Mellors, J. W. (2007) *AIDS* **21,** 1405–1414
19. Sluis-Cremer, N., Arion, D., Parikh, U., Koontz, D., Schinazi, R. F., Mellors, J. W., and Parniak, M. A. (2005) *J. Biol. Chem.* **280,** 29047–29052
20. Johnson, K. A. (1995) *Methods Enzymol.* **249,** 38–61
21. Tuske, S., Sarafianos, S. G., Clark, A. D., Jr., Ding, J., Naeger, L. K., White, K. L., Miller, M. D., Gibbs, C. S., Boyer, P. L., Clark, P., Wang, G., Gaffney, B. L., Jones, R. A., Jerina, D. M., Hughes, S. H., and Arnold, E. (2004) *Nat. Struct. Mol. Biol.* **11,** 469–474
22. Zinnen, S., Hsieh, J. C., and Modrich, P. (1994) *J. Biol. Chem.* **269,** 24195–24202
23. Gu, Z., Salomon, H., Cherrington, J. M., Mulato, A. S., Chen, M. S., Yarchoan, R., Foli, A., Sogocio, K. M., and Wainberg, M. A. (1995) *Antimicrob. Agents Chemother.* **39,** 1888–1891
24. Cherrington, J. M., Mulato, A. S., Fuller, M. D., and Chen, M. S. (1996) *Antimicrob. Agents Chemother.* **40,** 2212–2216
25. Meyer, P. R., Matsuura, S. E., So, A. G., and Scott, W. A. (1998) *Proc. Natl. Acad. Sci. U.S.A.* **95,** 13471–13476
26. Meyer, P. R., Matsuura, S. E., Mian, A. M., So, A. G., and Scott, W. A. (1999) *Mol. Cell* **4,** 35–43
27. Boyer, P. L., Sarafianos, S. G., Arnold, E., and Hughes, S. H. (2001) *J. Virol.* **75,** 4832–4842
28. Tong, W., Lu, C. D., Sharma, S. K., Matsuura, S., So, A. G., and Scott, W. A. (1997) *Biochemistry* **36,** 5749–5757
29. Deval, J., White, K. L., Miller, M. D., Parkin, N. T., Courcambeck, J., Halfon, P., Selmi, B., Boretto, J., and Canard, B. (2004) *J. Biol. Chem.* **279,** 509–516

Downloaded from www.jbc.org at KU Leuven - Biomedical Library, on April 19, 2010